Performance Analysis of a Three-Phase Induction Motor with Double-Triple Winding Layout

Mbika Muteba
Department of Power Engineering
Vaal University of Technology
Vanderbijlpark, South Africa
mbikam@vut.ac.za

Adisa A. Jimoh
Department of Electrical Engineering
Tshwane University of Technology
Pretoria, South Africa
jimohaa@tut.ac.za

***Abstract*— This paper presents the performance of three-phase induction motor with a stator winding comprising of a combination of double and triple layer arrangements in slots, here simply referred to as double-triple stator winding layouts. The proposed layout provides a three-phase induction motor with high torque density and greater efficiency than the conventional machine with double winding layout. Field analysis technique is used to show that this winding arrangement has improved harmonic content and the machine performance is computed using Finite Element Method (FEM). Saturation is accounted for in the computation of the inductances. A 1500 W conventional three-phase induction machine with 36 stator slots is first wound as a four-pole double layer and then as a four-pole double-triple layer for the experimental study. Both windings are chorded with one slot with same number of turns per phase and use the same squirrel cage rotor.**

I. INTRODUCTION

The airgap field distribution in induction motors (IMs) is influenced by the stator and rotor magneto-motive force (MMF) distribution and magnetic saturation in stator and rotor teeth and back cores. The placement of windings in slots leads to a stepped-like waveform of the stator or rotor MMFs which exhibit space harmonics [7]. Most electrical machine designs rely on the fundamental flux wave theory [2]. Attention is concentrated on the achievement of sinusoidal flux density in the airgap with a little harmonic content [1].

Conventional windings for poly-phase induction motors are layed out in one or two-layers in stator slots [7]. The total number of coils equals half the number of stator slots for single layer configurations and equal to number of stator slots in double-layer configurations. Full-pitched and short-pitched are used depending on the application. Windings are built with integer or fractional slots per pole and per phase [3], [4].

Moreover, the requirements of many applications both in industry and in the field of renewable energy conversion are though that traditional layouts are abandoned in favor of new topologies or new light is shed over older one [1]. In this work a new winding topology ideally suited for high phase order (hpo) and high powered induction machines is proposed, albeit tested for 1.5kW conventional three-phase induction machine to demonstrate its potentials.

The layout of this paper is such that the machine parameters are presented in section II following the introduction. This is followed by the machine design in section III. In section IV field analysis is made. The simulation results based on finite element analysis are presented in section V, and these are then corroborated by the results of the experimental works carried out in section VI. The paper ends with a conclusion in section VII.

II. MACHINE PARAMETERS

Since compared to the normal machine the only change here is the arrangement of the stator winding. The normal theory of the induction machine is applicable, hence the steady-state equivalent circuit, shown in fig.1.

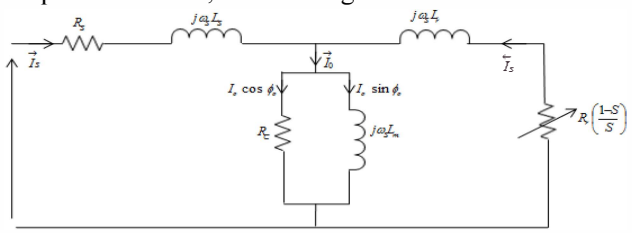

Fig.1. Steady-state equivalent circuit

Where: R_s and R_r are the stator and rotor resistances, L_s and L_r are the stator and rotor leakage inductances, L_m and R_c are the magnetizing inductance and resistance representing the core loss respectively, ω_s is the frequency angular velocity, s the p.u slip, ϕ_o is the phase shift between the stator voltage V_s and the no-load current I_o.

Since the machine equivalent circuit is the same, the usual tests - namely: no-load, locked rotor and dc resistance - were used to determine the machine parameters. Table I

978-1-4799-0073-2/13/$31.00 ©2013 IEEE

gives the parameters of the conventional and the proposed machine.

TABLE I
MACHINES PARAMETERS

Description	R_s	R_r	X_s	X_r	X_m	R_c
Conventional	8.90Ω	7.62Ω	15.08Ω	15.08Ω	195.33Ω	1723Ω
Proposed	8.80Ω	7.94Ω	14.24Ω	14.24Ω	197.85Ω	1693Ω

III. MACHINE DESIGN

The proposed double-triple layer configuration has in some slots conductors belonging to two different phases where one phase is made of a half coil and the other phase is made of one and a half coil. The currents in these phases are out of phase with one another by either 2π/3 electrical radians or 4π/3 electrical radians. Consequently, the net currents and leakage flux are less than in the slots with the current belonging to the same phase. Fig.2 illustrates the double-triple layer configuration, and it is noted that the phase band of the proposed double-triple configuration consists now of four slots, not three slots as in the conventional double layer winding. Therefore, the new phase-belt spread is 4π/9 electrical radians.

Furthermore, it is noted that the four slots of the new phase-belt spread accommodate conductors that carry currents belonging to all the three phases.

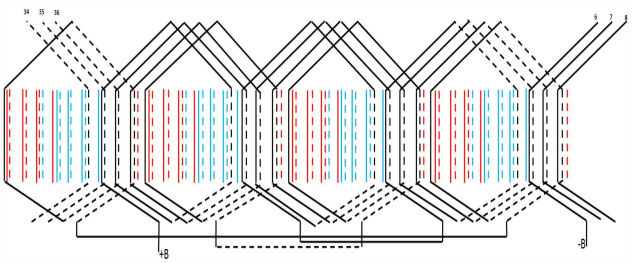

Fig.2. Proposed double-triple winding layout, only coils for phase B are shown.

The process of the stator design starts with the winding design. After selecting a proper value for number of slots per phase per pole, q, to obtain an approximate sinusoidal MMF distribution [7], the number of turns can be determined. Conventional windings for poly-phase induction machines are layed out in one or two-layers in stator slots. The total number of coils equals half the number of stator slots for single layer configurations and equal to number of stator slots in double-layer configurations. Full-pitches and short-pitched are used depending on the application. Single-layer windings are built with unity coil pitch, thus the pitch factor is unity [7].

The general expressions for harmonic distribution factor and harmonic chording factor are given by (1) and (2) respectively. For distributed winding, coil span is π electrical radian.

$$K_{dnC} = \frac{\sin nq(\alpha_s/2)}{q \sin n(\alpha_s/2)} \quad (1)$$

$$K_{pnC} = \sin n(\pi y/2\tau) \quad (2)$$

Where: K_{dnC} is the harmonic "n" distribution factor of conventional single or double layer winding, K_{pnC} is the harmonic "n" pitch factor of conventional chorded double layer winding and the ratio y/τ is the coil span and α_s is the slot pitch angle in electrical radians.

It was indicated earlier that in the proposed winding configuration, the coils were accommodated in the four slots that comprised the phase-belt band had different field component magnitudes. Two slots housed half-coil each and the other two slots housed a full coil each. The harmonic "n" distribution factor of the proposed double-triple layer configuration is than calculated by also taking into consideration the difference in slot field's component. Consequently, the harmonic distribution factor is denoted as in (3) and the winding factor is the product of (2) and (3).

$$K_{dn2} = \frac{\sin n(q_i + q_j)(\alpha_s/2)}{(q_i + q_j)\sin n(\alpha_s/2)} \quad (3)$$

Where: q_j is the number of slots per phase per pole that house half coil sides and q_i is the number of slots per pole per phase that house full coil sides only.

Table II displays the readily calculated harmonic winding factors for the conventional and proposed machines. It is noted that the conventional winding layout has a higher fundamental winding factor compared to the proposed winding topology, however, the later reduced the 5th, 11th, 13th, 17th and 19th harmonic winding factors. This could mean that the proposed winding topology has the edge of producing a higher average torque density.

TABLE II
HARMONIC WINDING FACTORS FOR THE CONVENTIONAL AND PROPOSED MACHINES

Description	1^{st}	5^{th}	7^{th}	11^{th}	13^{th}	17^{th}	19^{th}
Conventional	0.94	0.13	-0.06	-0.10	-0.13	-0.94	-0.94
Proposed	0.91	-0.07	-0.08	-0.08	-0.07	0.91	0.91

The prototype machine utilized an off the shelf 28 bar rotor. The rotor design entails the selection of the required number of rotor bars and the optimum skewing angle to get rid of effect of the undesired space harmonics. One of the main design considerations of the cage rotor induction motors is the selection of stator to rotor combination. A small change in the number of stator or rotor slots can create unacceptable audible noise or may even prevent the motor from starting at certain positions. The main reason for these phenomena is the parasitic torque by stator as well as rotor MMF [7]. To avoid producing parasitic torque, condition expressed in equation (4), extracted from [7], must be satisfied. The condition guarantees that the stator and rotor

MMFs do not co-exist. The prototype and simulated machines in this paper have 28 rotor bars. Table III indicates that the forward 13th stator harmonic MMF co-exists with the backward 13th rotor harmonic MMF.

$$6x_s + 1 \neq x_r \frac{N_r}{p_s} + 1$$
$$x_s = \pm 1, \pm 2, .. \; and \;\; x_r = \pm 1, \pm 2, ... \qquad (4)$$

The interaction between n_{+13} and μ_{-13} of air gap field components produces parasitic torques whose magnitude depends on the product of their magnitudes and the frequency depends on the difference between the speeds of these two fields. The speed of the slip between the n_{+13} and μ_{-13} is key in producing the parasitic torque. If the speed of slip is zero, the interaction between these two components will produce a zero parasitic torque.

TABLE III
RELATIONSHIP BETWEEN STATOR MMF HARMONICS ORDER AND ROTOR MMF HARMONICS

For x_r=-1						
Description	x_s= -1	x_s= -1	x_s= -1	x_s= -1	x_s= -1	x_s= -1
n_s	-5	+7	-11	+13	-17	+19
μ_r	-	-	-	-13	-	-

IV. FIELD ANALYSIS

A. Fourier Series of the winding function

The winding functions presented in this paper are odd periodic function $f(\theta)$ over interval $-\pi < \theta < \pi$, thus the Fourier series expansion of these periods will consist of sine terms only as in (5).

$$N(\theta) = \sum_{n=1,3,5...}^{\infty} N_n \sin(n\theta) \qquad (5)$$

Where: N_n is the harmonic winding coefficient and θ is the angular position in electrical degrees.
Such a winding, if carrying a current $i=i(t)$, will produce an MMF:

$$F = N(\theta) \times i = i \times \sum_{n=1,3,5..}^{\infty} N_n \sin(n\theta) \qquad (6)$$

The winding function is considered as equivalent to a series connection of windings having conductor distribution as:

$$N_1 \sin\theta, N_3 \sin 3\theta, N_5 \sin 5\theta \;\; etc \ldots \qquad (7)$$

The MMF acting across the air-gap associated with the stator current is:

$$F = F_A + F_B + F_C = N_A(\theta)\, i_A + N_B(\theta)\, i_B + N_C(\theta)\, i_C \qquad (8)$$

Where N_A, N_B and N_C are machine winding functions and compose of set of three-phase shifted square wave.

$$N_n = \frac{4}{\pi} \frac{N}{2p} (turns \;\; per \;\; pole) \qquad (9)$$

Where: N is the total number of turns per phase, thus the winding function is expressed as in (10).

$$N(\theta) = \frac{4}{\pi} \frac{N}{2p} \sum_{n=1,3,5}^{\infty} \frac{k_{Wn}}{n} \sin n\theta \qquad (10)$$

Where: k_{Wn} is the winding harmonic factor that depends on specific winding configuration as noted in table II.

B. MMF analysis using a Matlab function

In this sub-section, the MMF set up by the stator current is analyzed using a Matlab function. It is common to approximate the MMF of distributed windings as a stair case approximation to a sinusoidal. The prototype machines used in this paper have 4-pole and 36 stator slots, resulting in average 3 slots per pole per phase in either case. It is noted that for both windings, only 18 stator slots of the machines are shown.
In Fig. 3 and Fig. 4 are shown the conventional and proposed winding topologies, respectively. Where (a) is the winding cross section, (b) MMF winding function for stator phase "A" alone, (c) air gap MMF profile for phase "A" alone and (d) Fourier expansion of the air gap MMF profile. It is observed in Fig. 3 and Fig.4 that the first four phase-belt harmonics harmonic MMFs (5th, 7th, 11th and 13th) are greatly reduced from 9 % (5th), 2 % (7th), 1.8 % (11th) and 5 % (13th) for the conventional double layer winding down to 1.8 % (5th), 0.2 % (7th), 0.2 % (11th) and 0.8 % (13th) for the proposed double triple layer winding. The combination of double and triple configurations has the edge to reduce the two unwanted first phase-belt MMF harmonics (5th and 7th) in a three-phase IM.

V. FINITE ELEMENT MODEL

In recent years the Finite Element Method becomes widely used in the design and analysis of electrical machines. In this paper the FEM models are analyzed in nonlinear magneto-static problem based on the well-known Poisson's equation for vector magnetic potential ***A (B=curl A)***. The Poisson's equation of the planar model is given by (11).

$$\frac{\delta}{\delta x}\left(\frac{1}{\mu_y}\frac{\delta A}{\delta x}\right) + \frac{\delta}{\delta y}\left(\frac{1}{\mu_x}\frac{\delta A}{\delta y}\right) = -j + \left(\frac{\delta H_{cy}}{\delta x} - \frac{\delta H_{cx}}{\delta y}\right) \qquad (11)$$

Where: "***B***" is the magnetic flux density and the vector of the magnetic flux density components are as in (12).

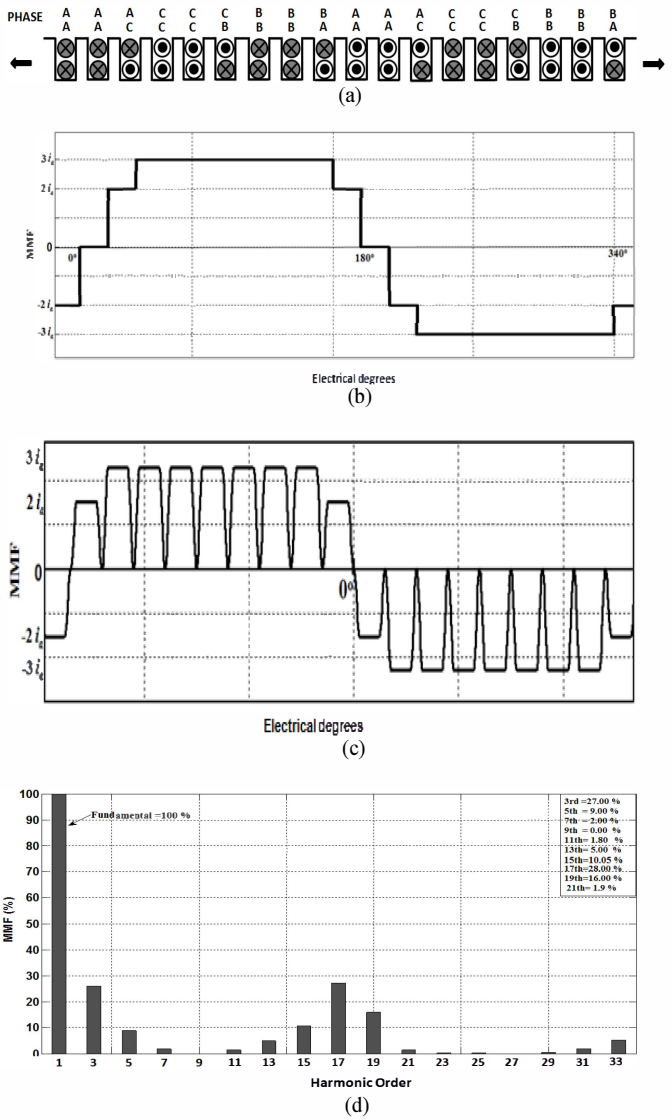

Fig.3. Three-phase conventional double layer winding, (a) winding cross section, (b) MMF winding function for phase A, (c) the air gap MMF profile for phase A, and (d) the Fourier expansion of the air gap MMF profile

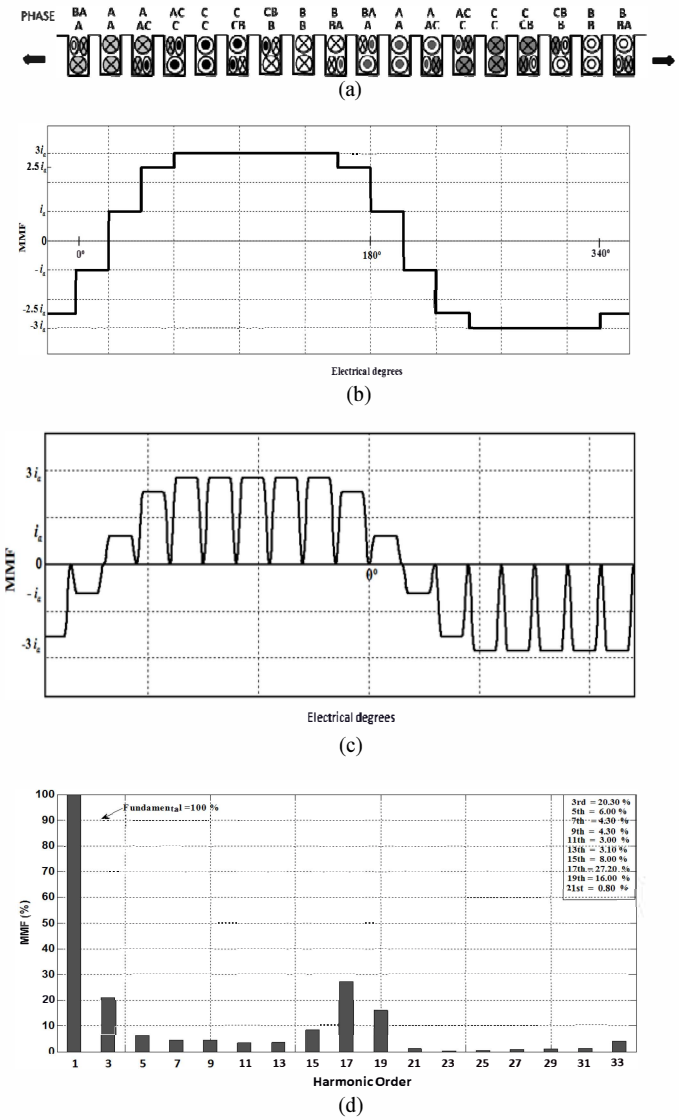

Fig.4. Three-phase proposed double triple layer winding, (a) winding cross section, (b) MMF winding function for phase A, (c) the air gap MMF profile for phase A, and (d) the Fourier expansion of the air gap MMF profile

$$B_x = \frac{\delta A}{\delta y} \qquad (12)$$

Where: μ_x *and* μy are the components of the magnetic permeability, H_{cx} and H_{cy} are the components of the coercive force vector and j is the current density within each block of the model.

The flux density is assumed to lie in the plane of the model (x, y). The space current is described by the total number of ampere turns associated with the block density associated with their block. Dirichlet boundary conditions with zero vector potential are set to the outer stator and inner rotor shaft of the machine models. By doing so the solution is confined inside the machine frame [4] . A two dimensional Cartesian-coordinate area are modeled with "x" number of nodes of mesh. Fig.5 and Fig.6 illustrate the FEM of the phase distribution in slots and magnetic field lines for the conventional and proposed IMs.

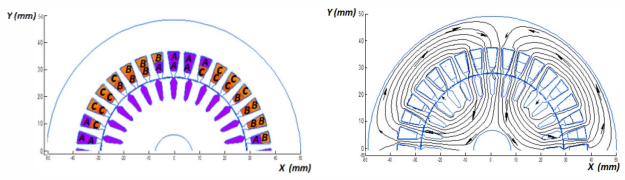

Fig.5. Finite Element Model of the conventional three-phase IM. (a) Phase distribution in slots. (b) Magnetic field lines

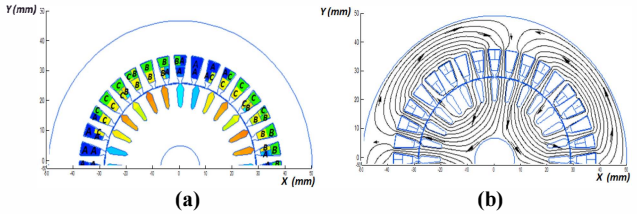

(a) (b)

Fig.6. Finite Element Model of the proposed three-phase IM with double-triple layer winding. (a) Phase distribution in slots. (b) Magnetic field lines

VI. EXPERIMENTAL EVALUATION

This section presents the summary of the main experimental results conducted on the prototype machines. In Fig.7 (a) and (b) torque speed and torque current characteristics of the prototype proposed machine are compared with the torque speed and torque current characteristics of the conventional machine. It is noted that at rated speed (1420 r.p.m) the proposed double triple layout machine has a higher torque magnitude than the conventional machine. The experimental power factor and efficiency of the prototype conventional double layer and proposed double-triple layer machines are provided in Fig.8 (a) and (b). It is noted that at rated power (1500 W) the proposed machine reaches a lagging power factor of 0.9. Observing Fig.6 (b), it is evident that the proposed machine reaches the maximum efficiency of 84% when the machine output is 1000 W. On the other hand, the conventional machine has a maximum efficiency of 77% when the output is 710 W.

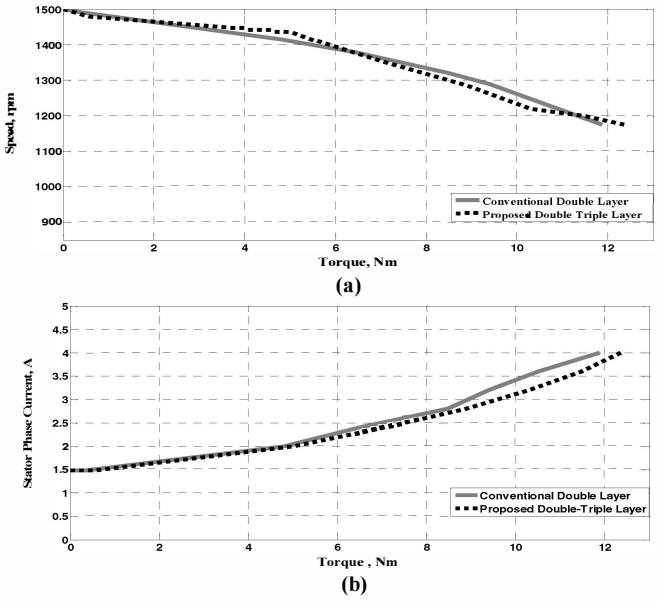

Fig.7 Conventional and proposed machines. (a). Experimental speed-torque characteristics, (b) Experimental stator current-torque characteristics

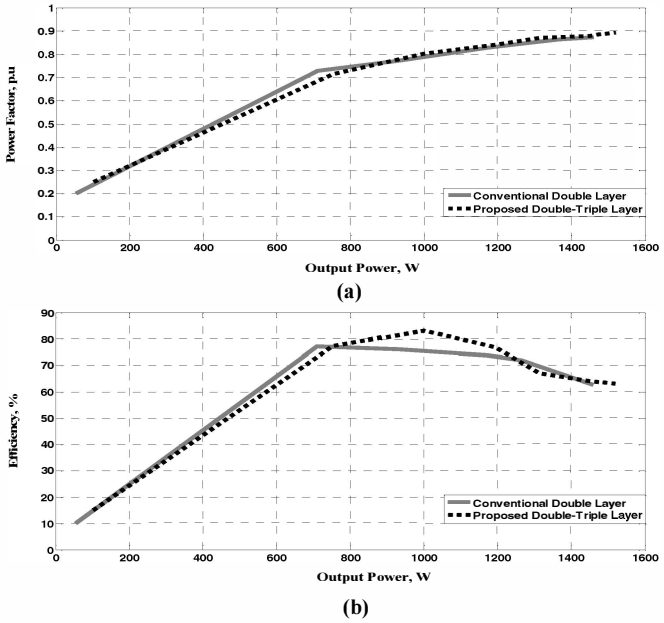

Fig.8. Comparison between conventional and proposed IMs. (a) Experimental power factor as function of output power, (b) Experimental efficiency as function of output power

In Fig.9 the efficiency and the power factor of the prototype machines are presented as function of slip. On the other hand Fig. 10 illustrates the comparison between experimental and simulation speed torque characteristics of the convention and proposed IMs.

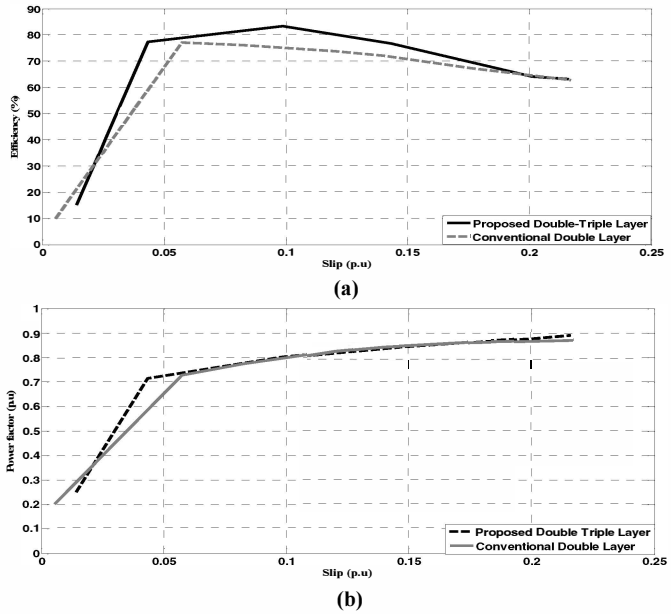

Fig.9. Comparison between conventional and proposed IMs (a) experimental efficiency as function of slip, (b) Experimental power factor as function of slip.

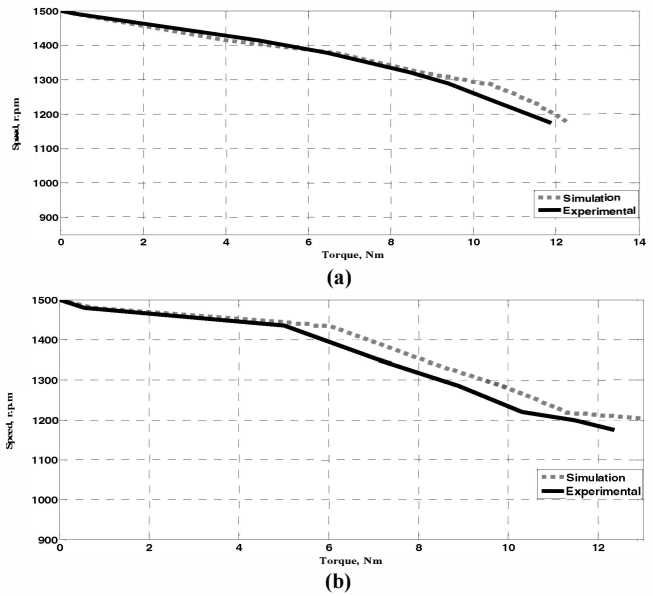

Fig.10. Comparison between simulation and experimental result of the torque speed characteristics: (a) Conventional machine, (b) proposed machine.

It is observed in Fig.9 (a) that the proposed IM provides high efficiency compared to the conventional machine in the zone of operation between 0.026 p.u of slip and 0.18 p.u of slip. At rated speed of 1420 rpm that correspond to a slip of 0.053, the efficiency is observed to be at 78 % for the proposed machine and at 72% for the conventional machine. On the other hand the power factor illustrated in Fig.9 (b) as a function of slip is 0.74 lagging at slip of 0.053 for the proposed IM and 0.68 lagging for the conventional IM at the same operating point.

VII. CONCLUSION

The performance of three-phase induction motor with proposed double-triple layer configuration has been analyzed. The experimental electrical and mechanical characteristics of the IM with proposed double-triple layer configuration have been compared to those of the IM with conventional double layer winding. It is demonstrated through results obtained from measurements that the proposed machine has the edge of producing high torque density and delivering an output with greater power factor and efficiency as compared to the conventional machine. A comparison between the simulation and experimental torque speed characteristics of three-phase induction motor with proposed layout and conventional layout has been presented. A good correlation has been noted between the experimental and simulation results.

The proposed idea in this paper means that the designer needs to make provision for enough space in the slots to accommodate insulation and avoid creating big space between coil sides in a slot.

Although, the prototype machines used in this paper are low power IMs, the idea of the proposed winding topology is destined for High Phase Order application to high power rating IMs. The use of the proposed winding topologies in low power IMs still needs to be investigated to find out if this idea makes economic sense, as the cost to design the winding combined with the cost to execute the winding should not be more than the cost of the conventional double layer winding.

Further study will look at the magnetic loading capability of the proposed winding topologies, details about the iron losses, stator copper losses, and mechanical and stray load losses.

REFERENCES

[1] Ayman S. Abdel-Khalik and Shehab Ahmed, "Performance evaluation of a five-phase modular winding induction machine", *IEEE Trans, on Industrial Applications*, Vol.59. No.6, pp. 2654-2669, June. 2012.

[2] E. A. Klingshirm, "High phase order induction motors part 1-description and theoretical considerations", *IEEE Trans. Power Apparatus and Systems*, vol. PAS-102, No, Jan 1983.

[3] A.M. EL-Refaie,"Fractional-slot concentrated-windings synchronous permanent magnet machines: Opportunities and challenges," *IEEE Trans. Ind. Electron.*, Vol.57.No.3, pp. 107-121, May/June, 2010.

[4] J.A. Güemes, A.M. Iraolagoitia, P.Fernández and M.P Donsión, "Comparative study of PMSM with integer-slot and fractional-slot windings. IEEE, XIX International Conference on Electrical Machines-ICEM2010, Rome.

[5] L.A. N. Pereira, C.C. Scharlau, L.F. A Pereira, and J. F Haffner, "General model of a five-phase induction machine allowing for harmonics in the airgap field". *IEEE Trans, Energy Convers*, Vol.21. No.4, pp. 891-899, Dec. 2006.

[6] A. Abdel-Khalik, M. Masoud, and B. W. Williams, "Eleven-phase induction machine: Steady-state analysis and performance evaluation with harmonic injection," *IET Elect. Power Appl.*, Vol.4.No.8, pp. 670-685, Sept, 2010.

[7] I. Boldea and S. Nasar, *The induction Machine Handbook*. Boca Raton, FL: CRC, 2002.